ORIGINAL ARTICLE

Karyometry detects subvisual differences in chromatin organisation state between non-recurrent and recurrent papillary urothelial neoplasms of low malignant potential

M Scarpelli, R Montironi, L M Tarquini, P W Hamilton, A López Beltran, J Ranger-Moore, P H Bartels

J Clin Pathol 2004;**57**:1201–1207. doi: 10.1136/jcp.2004.017608

See end of article for authors' affiliations

Correspondence to: Professor R Montironi, Section of Pathological Anatomy and Histopathology, Polytechnic University of the Marche Region (Ancona), School of Medicine, Umberto I Hospital, Via Conca, 71, I-60020 Torrette, Ancona, Italy; r.montironi@univpm.it

Accepted for publication 1 June 2004

Aim: To analyse nuclear chromatin texture in non-recurrent and recurrent papillary urothelial neoplasms of low malignant potential (PUNLMPs).

Materials: Ninety three karyometric features were analysed on haematoxylin and eosin stained sections from 20 PUNLMP cases: 10 from patients with a solitary PUNLMP lesion, who were disease free during at least eight years' follow up, and 10 from patients with unifocal PUNLMP, one or more recurrences being seen during follow up.

Results: Kruskal-Wallis analysis was used to search for features showing significant differences between recurrent and non-recurrent cases. Significance was better than $p<0.005$ for more than 20 features. Based on significance, six texture features were selected for discriminant analysis. Stepwise linear discriminant analysis reduced Wilk's λ to 0.87, indicating a highly significant difference between the two multivariate data sets, but only modest ability to discriminate (70% correct case classification). A box sequential classifier was used based on data derived from discriminant analysis. The classifier took three classification steps and classified 19 of the 20 cases correctly (95% correct case classification). To determine whether significant case grouping could also be obtained based on an objective criterion, the merged data sets of non-recurrent and recurrent cases were submitted to the unsupervised learning algorithm P-index. Two clusters were formed with significant differences. The subsequent application of a Cooley/Lohnes classifier resulted in an overall correct case classification rate of 85%.

Conclusions: Karyometry and multivariate analyses detect subvisual differences in chromatin organisation state between non-recurrent and recurrent PUNLMPs, thus allowing identification of lesions that do or do not recur.

The World Health Organisation/International Society of Urological Pathology consensus classification of urothelial (transitional cell) neoplasms of the urinary bladder[1] subdivides the morphological spectrum of non-invasive urothelial papillary tumours into papilloma, papillary urothelial neoplasm of low malignant potential (PUNLMP), low grade papillary carcinoma, and high grade papillary carcinoma. This classification, known as the 1998 WHO/ISUP classification, will become the 2004 WHO classification of the non-invasive papillary urothelial tumours. It replaces the 1973 WHO system, which included urothelial papilloma, and papillary carcinoma of grade 1, grade 2, and grade 3.[2] PUNLMP basically corresponds to papillary carcinoma of grade 1.[3] There is no full consensus in the current literature on whether the 1973 WHO system should be discarded and replaced by the 1998 WHO/ISUP classification.[4 5]

PUNLMP is a non-invasive papillary urothelial lesion with an orderly arrangement of cells within papillae, with minimal architectural abnormalities and minimal nuclear atypia, irrespective of cell thickness.[1] In general, the major distinction from papilloma is that in PUNLMP the urothelium is much thicker and/or nuclei are greatly enlarged. In contrast, urothelial papilloma has no architectural or cytological atypia. Mitotic figures are infrequent in PUNLMP, and usually limited to the basal layer. Low grade papillary urothelial carcinoma is characterised by an overall orderly appearance, but with easily recognisable variations in the architectural and or cytological features, even at scanning magnification.[6] Variations in polarity and nuclear size, shape, and chromatin texture comprise the minimal but definitive cytological atypia. Mitotic figures are infrequent and are usually seen in the lower half.[5]

> "It is not possible to identify those papillary urothelial neoplasm of low malignant potential cases that will recur based on conventional histopathological assessment"

PUNLMP is a clinically important lesion because patients are at increased risk of developing a recurrence. This was documented in 35% and 47% of patients reported by Holmäng and colleagues[7] and by Pich *et al*,[8] respectively. Nevertheless, the prognosis for patients with PUNLMP is excellent. Rarely, these patients may present with tumour progression; that is, a tumour recurrence with invasion of either the lamina propria or the muscularis propria, or carcinoma in situ. In a series of 112 patients described by Cheng *et al*,[9] only four developed invasive urothelial carcinoma, whereas Samaratunga *et al* reported a progression rate of 8%, compared with 0% and 13% for papilloma and low grade papillary carcinoma, respectively.[10]

It is not possible to identify those PUNLMP cases that will recur based on conventional histopathological assessment.[11]

Abbreviations: CK, cytokeratin; CLASIF, Cooley-Lohnes classifier; H&E, haematoxylin and eosin; ISUP, International Society of Urological Pathology; NR, non-recurrent; OD, optical density; PUNLMP, papillary urothelial neoplasms of low malignant potential; R, recurrent; WHO, World Health Organisation

Table 1 Sample list of features used in our study

- Total optical density (feature number 001)
- Nuclear area (feature number 002)
- Variance of optical density (OD) values (feature number 006)
- Pixel OD histogram (0.2–0.3 bin) (feature number 010)
- Run length feature (OD, 0.0–0.3, 1–2 pixels) (feature number 267)
- Run length feature (OD 0.3–0.6, 3–4 pixels) (feature number 274)
- Percentage of long runs (feature number 304)
- Grey level non-uniformity (feature number 305)
- Run length non-uniformity (feature number 306)
- Percentage of pixels occurring in a run (feature number 307)
- Mean OD value (feature number 317)
- OD value 20% above mean OD (feature number 318)
- Total number of very dark pixels (feature number 319)
- Total number of light pixels (feature number 320)

The values in parenthesis refer to an arbitrary code number with which the feature is identified in the computer program.

A variety of immunohistochemical and molecular markers have been applied to predict disease recurrence.[12–15] However, conflicting results have been reported. Recent studies have shown that evaluation of the nuclear chromatin organisation state by karyometry is useful in the identification of patients at risk for recurrence of superficial urothelial carcinoma.[16–17] To the best of our knowledge there are no previous studies on the usefulness of karyometry in the identification of those PUNLMP cases that will recur.

The goal of our study was to analyse nuclear chromatin texture in non-recurrent and recurrent PUNLMP.

MATERIALS AND METHODS

Twenty cases of PUNLMP were retrieved from the tissue archives of the section of pathological anatomy and histopathology, Polytechnic University of the Marche Region, Ancona, Italy. Ten were from patients who had a solitary lesion, less than 1 cm in diameter, diagnosed as PUNLMP. The patients were disease free during a follow up period of at least eight years. This group was defined as "non-recurrent" (NR). The other 10 were from patients with a unifocal lesion, less than 1 cm in diameter, diagnosed as PUNLMP, with one or more recurrences being seen in the follow up (none of the these cases progressed to a higher grade and/or became invasive. In most of the patients the first recurrence was seen six months to one year after the removal of the primary tumour; the case with ambiguous classification—see Results—recurred after one year and a half). This group was defined as "recurrent" (R). The recurrent lesions showed a histological appearance identical to that seen at the first presentation. From this group, only the primary or initial tumours were included in the investigation. There were no differences between the NR and R groups with regard to sex and age of the patients (their mean age was 62.5 years). The initial tumours and the recurrences were treated by transurethral resection. None of the patients received adjuvant treatment—for example, BCG or intravesical chemotherapy.

All the samples had been fixed in 4% buffered formaldehyde for 24 hours before processing and originally reported according to the 1973 WHO system. We are in the process of reclassifying all the bladder specimens seen in Ancona since 1990, and this is being done by two of our group (RM and LMT) according to the 1998 WHO/ISUP classification.

Karyometric and statistical analyses

For the purpose of our study, 5 µm thick sections were cut from the paraffin wax blocks and stained with haematoxylin and eosin (H&E) in the same batch and at the same time.

Karyometry was carried out at the optical sciences centre of the University of Arizona, Tucson, Arizona, USA, on the fresh H&E stained sections. H&E staining was used so that the results from image analysis could be directly compared and correlated with the histopathological assessment. Bahr and colleagues[18] and Keenan and colleagues[19] showed that data derived from H&E and Papanicolaou stains are linearly correlated with those from Feulgen.

The nuclei were recorded on a video microscope equipped with a 63:1 Zeiss (Oberkochen, Germany) planapochromatic oil immersion objective, NA 1.40, and a COHU (San Diego, California, USA) black and white video camera. An interference filter with a maximum bandpass at 610 nm was used

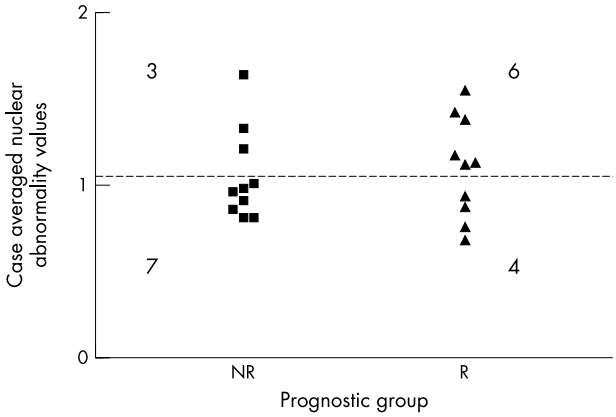

Figure 1 The case averaged nuclear abnormality values for two prognostic groups. An arbitrary threshold of approximately 1.05 can correctly classify 13 cases (65%) into the correct groups. NR, non-recurrent group; R, recurrent group.

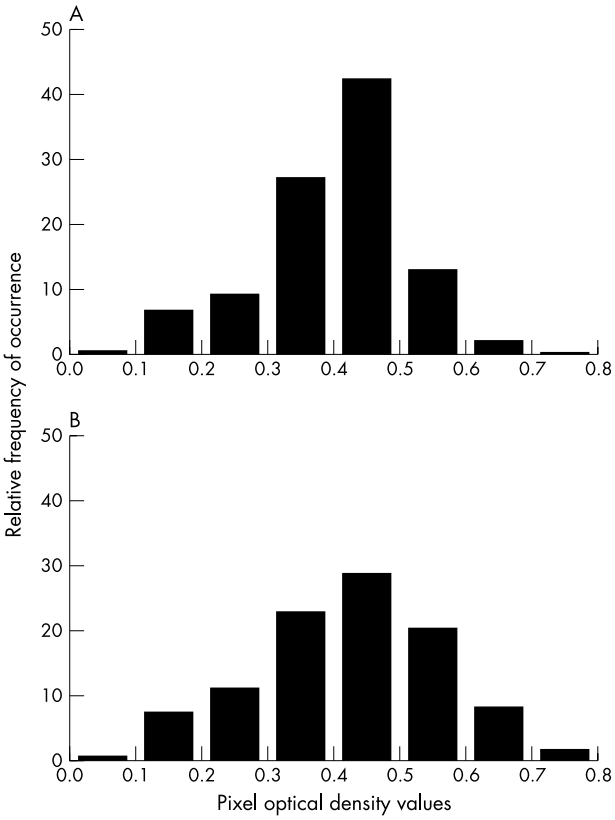

Figure 2 Pixel optical density histograms. There is a slight shift towards higher values in the recurrence data set; that is, there are denser chromatin granules. (A) Non-recurrent cases, (B) recurrent cases.

to enhance the contrast of the H&E stained sections. The relay optics provided a sampling density of 6 pixels/μm. Individual nuclei from the images were edited using an interactive procedure and then filed for feature extraction. Enough fields were recorded to provide 100 nuclei/case for a total of 2000 nuclei. The nuclei were randomly selected from the intermediate and basal layers.

In total, 93 karyometric features were analysed in our study. These were related to nuclear area, total optical density, and chromatin distribution and pattern.[20–22] Table 1 provides a sample list of the features analysed (all features are given in relative units of measure; the values in parenthesis refer to an arbitrary code number with which the feature is identified in the computer program).

Statistical analysis included the Kruskal-Wallis (KW) test to determine significant differences in the global (see below) and chromatin texture features between the two pathological groups. The available statistical power for assessing the accuracy of classification procedures was determined using nQuery 4.0 (Elashoff JD. *nQuery Advisor® Version 4.0*. Los Angeles, CA, 2000). Discriminant analysis was adopted to identify suitable subsets of features useful for the discrimination and classification of pathological groups (Elashoff JD. *nQuery Advisor® Version 4.0*. Los Angeles, CA, 2000).[23–27] The non-supervised learning algorithm P-index was used to explore multivariate data structure in pathological subgroups.[24] Statistical analyses also included the application of a box sequential classifier and a Cooley/Lohnes classifier (CLASIF) (Elashoff JD. *nQuery Advisor® Version 4.0*. Los Angeles, CA, 2000).[23–27] Significance of classification accuracy for each approach relied on exact binomial tests of significance performed using Stata 8.2.[26]

The sequential box classifier is a non-parametric procedure, which sequentially selects the features according to their ability to provide error free classification. After each step, the correctly classified objects are removed from further consideration, and the process is started again, searching for the best feature to work on the remaining subset of objects.[24]

CLASIF is a parametric procedure, which classifies objects on the basis of the highest relative likelihood into one of several possible multivariate probability density distributions. In our study, the non-supervised learning algorithm P-index formed two groupings of objects; that is, strictly on the basis of the data structure of the merged NR and R data sets. The P-index established mean vectors and variance–covariance matrices for these groupings. These were then submitted to the CLASIF algorithm.[27]

Although there were 1000 nuclei in each group, there were only 10 cases in each group. This was deemed inadequate to form independent training and test data sets on a case basis. To guard against overtraining and the potential inclusion of a spuriously discriminating feature, it was decided to set the feature selection criterion to the high significance level of $p < 0.005$.

Table 2 Scaled frequencies of occurrence for the non-zero elements in the co-occurrence matrix

Element	NR	R
1.1	195.5	214.2
1.2	52.3	49.6
1.3	0.4	1.24
2.2	614.8	458.7
2.3	17.3	26.6
2.4	0.01	0.01
3.3	49.5	166.8
3.4	0.11	1.32
4.4	0.04	2.56

NR, non-recurrent group; R, recurrent group.

Table 3 The run length frequencies in the lower pixel OD ranges up to OD 0.60, the OD ranges 0.60–0.90, 0.90–1.20, and 1.20–1.50

OD range	Run lengths	Relative frequencies	
		NR	R
0.60–0.90	1–2	7.5	10.3
	3–4	2.2	4.3
	5–6	1.2	2.6
	7–8	0.7	1.9
	9–10	0.4	1.3
	11–12	1.2	5.8
0.90–1.20	1–2	0.07	0.5
	3–4	0.002	0.17
1.20–1.50	1–2	0.002	0.008

OD, optical density; NR, non-recurrent group; R, recurrent group.

RESULTS

Nuclear abnormality and lesion signature

As a first step, nuclear abnormality values were computed, using as normal reference data set nuclei from normal bladder epithelium, recorded in an earlier study[16] (for details in the calculation of the nuclear abnormality value, see Montironi and colleagues[16] and Bartels and colleagues[28]). In most cases, the nuclear abnormality was only slightly increased over the values expected for a set of normal nuclei—that is, 0.65. Figure 1 shows the case averaged nuclear abnormality values for two prognostic groups. An arbitrary threshold of 1.05 can correctly classify 13 cases (65%) into correct groups. The distributions of nuclear abnormality values—the lesion signatures—show a slight increase of nuclei with higher abnormalities in the data set representing recurrent disease. However, the difference is too small to offer discriminating information.

Global features

The features expressing values descriptive of the nucleus as a whole, the so called global features—nuclear area, nuclear roundness, and total optical density—did not show significant differences between the non-recurrent and recurrent cases.

Chromatin phenotype

The pixel optical density (OD) histogram showed a slight shift towards higher values in the recurrent data set (fig 2). The pixel OD co-occurrence features showed a similar trend. Table 2 lists the scaled frequencies of occurrence for the non-zero elements in the co-occurrence matrix (the notation is row/column of a 6 × 6 pixel OD range matrix covering the

Table 4 Mean values of the six texture features used in the discriminant analysis

Features	NR	R
011	42.3	28.9
033	614.8	458.6
278	28.5	18.3
284	1.21	5.8
304	13.07	11.4
320	724.2	648.6

The features are represented by the value used to identify them in the computer program (the pixel OD histogram, the co-occurrence matrix, run lengths, and two summarising features).
OD, optical density; NR, non-recurrent group; R, recurrent group.

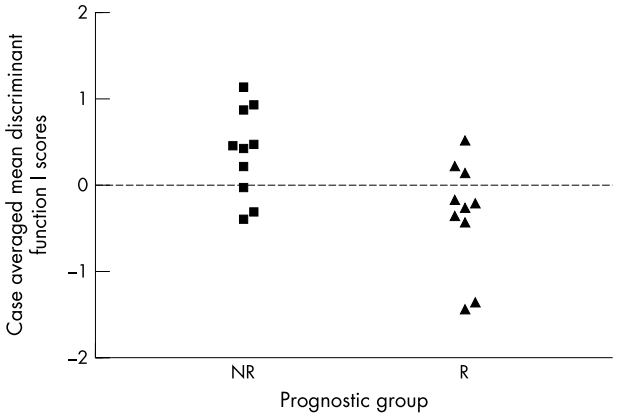

Figure 3 The case averaged discriminant function I scores for the prognostic groups. With a threshold of zero, 14 of the 20 cases are correctly classified. NR, non-recurrent group; R, recurrent group.

OD range from 0.0 to 1.8 and above).[22] In the recurrence data set there was an increase in pixel adjacencies in the 0.60–0.90 and 0.90–1.20 OD ranges—at higher OD values—suggesting denser and slightly larger chromatin granules.

The run length features reflected the same development in the two groups. Although there was almost no difference in the run length frequencies in the lower pixel OD ranges up to OD 0.60, the OD ranges 0.60–0.90, 0.90–1.20, and even 1.20–1.50 and higher, showed more and longer runs in the recurrence data set—granules were not only darker, but larger (table 3).

To search for specific features showing significant value differences, a KW test was conducted. The test showed more than 20 features with a level of significance better than $p < 0.005$. On the basis of their significance value, six texture features were selected for discriminant analysis. Table 4 lists these features, along with their mean values.

Discriminant analysis

A stepwise linear discriminant analysis reduced Wilk's λ to 0.87, indicating a high level of significance of the difference between the two multivariate data sets, but only a modest ability to discriminate: only 14 cases (seven of 10 in the NR group and seven of 10 in the R group) were correctly classified. A two sided exact binomial test results in a p value for this outcome of 0.115 when compared with the null hypothesis of no classification ability (a 50% classification rate by chance alone). Thus, if discriminant analysis had no ability to classify these cases, accuracy as high as this or higher would be observed by chance only one time in nine.

Figure 3 shows the case averaged discriminant function I scores for the two prognostic groups. The distribution of the scores showed a noticeable shift to negative values for the cases with recurrent lesions (assigned by the algorithm to the recurrent data set), and a reduction of the number of nuclei with high discriminant function scores, compared with the nuclei from non-recurrent cases (fig 4).

An attempt was made to use as a metafeature the percentages of nuclei above an arbitrary threshold in the discriminant function I score distribution. Such a threshold was set at a value of +0.40 (fig 4A). If one chose as a criterion the occurrence of 50% of nuclei above this threshold, the cases with more than 50% of nuclei above +0.40 are assigned to the NR group, whereas those cases with a proportion lower than 50% are assigned to the R group. Seven of the 10 non-recurrent cases and all 10 of the recurrent cases were correctly identified (85% correct classification; $p = 0.021$). This metafeature, which shows significance in its classifying ability, provides a good first step for a sequential classification procedure.

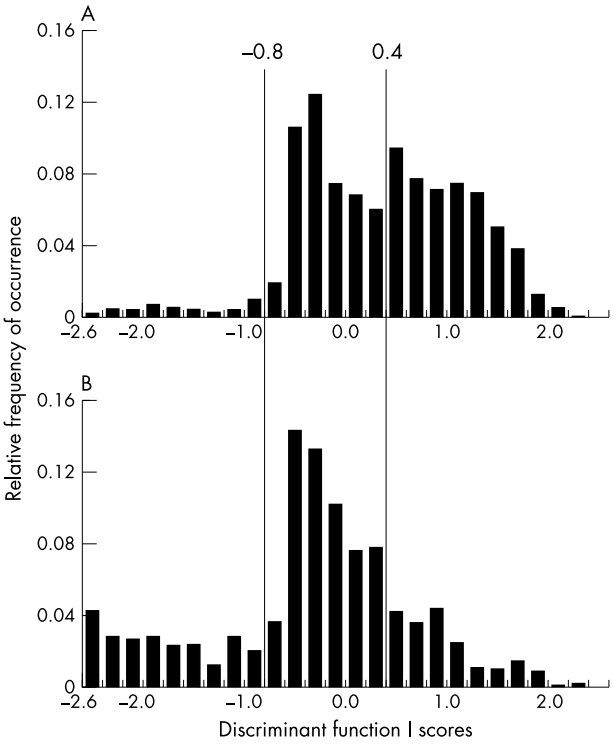

Figure 4 Distribution of discriminant function I scores. There is a noticeable shift to negative values for the cases with recurrent lesions (assigned by the algorithm to the recurrent data set), and a reduction of the number of nuclei with high discriminant function scores, compared with the nuclei from non-recurrent cases. (A) Non-recurrent cases, (B) recurrent cases.

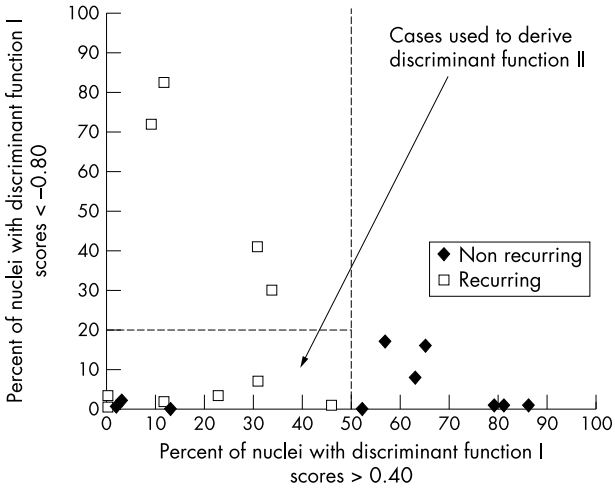

Figure 5 A threshold set at > 20% along this metafeature would allow error free recognition of four of the recurring cases, as opposed to the three non-recurrent cases with fewer than 50% of nuclei above the high threshold of +0.40.

In the data set of recurrent cases the percentage of nuclei with high negative values (discriminant function score of less than −0.8) was clearly increased (fig 4A,B). As a step in a sequential decision process, a threshold set at > 20% along this metafeature would allow an error free recognition of four of the recurring cases, as opposed to the three non-recurrent

Table 5 Mean discriminant function II scores

NR	R
0.415†	−1.360†
−1.561*	0.094†
−1.463*	−0.944†
−1.220*	−1.597†
−1.024*	0.766
−0.733*	−0.410†
−1.590*	−1.760†
−1.310*	0.108†
0.680†	−1.490†
0.650†	−1.670†

*Those cases unequivocally classified already by the percentage of cases above threshold on the discriminant function I score axis; †those cases correctly classified by the second step.
NR, non-recurrent group; R, recurrent group.

cases with fewer than 50% of nuclei above the high threshold of +0.40. Figure 5 shows this situation. In the lower left hand corner of this figure, there are nine cases that discriminant function I score metafeatures were unable to distinguish. These two sets of nuclei, of sample sizes 600 and 300, respectively, were subjected to a KW test to explore whether features with clearly different values existed. The KW test revealed more than 20 such features at a p value of 0.005 each. On the basis of their significance value, six features were selected for a discriminant run. Although the differences between the two multivariate data sets were not substantial, they were sufficient to allow a reduction of Wilk's λ to 0.83.The discriminant function II, derived from the nine cases, was then applied to all non-recurrent and recurrent cases. Table 5 shows the resulting mean discriminant function II scores. The dagger symbol in this table indicates those cases that were correctly classified by the second step (threshold on discriminant function I set at > 0.20).

A box sequential classifier (for specific details of this classifier see Bartels and Olson[24]) was used. This classifier took three classification steps and classified 19 of the 20 cases correctly (95%; $p < 0.0001$), deciding that for one case no unambiguous classification decision could be reached (table 6).

Unsupervised learning algorithm P-index and CLASIF

To determine whether a significant grouping of cases could be obtained based on an objective criterion, the merged data sets of non-recurrent and recurrent cases were submitted to the unsupervised learning algorithm P-index. The two features used previously were used again. The P-index formed two clusters with significant differences ($p = 0.037$), assigning 12 cases to the first cluster and eight cases to the second cluster (table 7).

Because the P-index algorithm forms its groupings based on estimates of the variance–covariance structure of the

Table 6 Results of the box sequential classifier

	NR correct	NR error	R correct	R error
Step1: discriminant I feature	7	0	0	0
Step 2: discriminant II feature	0	0	9	0
Step 3: discriminant I feature	3	0	0	0
Correctly classified	10		9	
Unclassified			1	

NR, non-recurrent group; R, recurrent group.

Table 7 The two clusters formed by the unsupervised learning algorithm P-index

Case no. (NR)	Cluster ID	Case no. (R)	Cluster ID
1	1	11	1
2	1	12	2
3	2	13	2
4	1	14	2
5	1	15	2
6	1	16	2
7	1	17	2
8	1	18	2
9	1	19	1
10	1	20	1

NR, non-recurrent group; R, recurrent group.

emerging clusters,[16 25] these results suggested that an estimate of a more generally valid classification success rate is offered by a bivariate plot, showing the discriminant function I derived feature on the abscissa and the discriminant function II score derived feature on the ordinate. This is depicted in fig 6, with the 95% confidence ellipses for the mean vectors and the 90% tolerance ellipses for the cases being shown. The Bayesian decision boundary delineates the line of equal error probability.

A numerical estimate of expected errors from this graph could be derived, but the application of a CLASIF, based on an estimate of the bivariate mean values and variance/covariance matrices, is more reliable.[27] This algorithm resulted in an overall correct case classification rate of 85% ($p = 0.021$).

DISCUSSION

Recurrence in PUNLMP has been investigated in relatively few studies.[11–15] Some of these were based on morphological evaluation and did not identify histological differences between recurrent and non-recurrent tumours. This holds true also for our study. Architectural and cellular differences

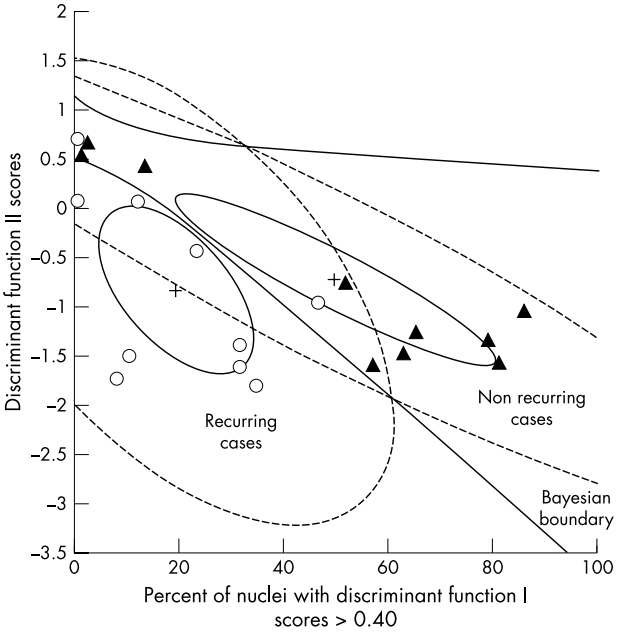

Figure 6 P-index algorithm groupings submitted to a Cooley-Lohnes classifier.The 95% confidence ellipses for the mean vectors and the 90% tolerance ellipses for the cases are shown. The Bayesian decision boundary delineates the line of equal error probability.

between the recurrent and non-recurrent lesions were not seen microscopically when the cases were reviewed.

Some studies investigated the cytokeratin (CK) expression pattern in recurrent and non-recurrent PUNLMP.[11 29–31] CK20 was the most commonly studied cytokeratin, either for normal (staining restricted to superficial or umbrella cells) or abnormal expression (diffuse full thickness positivity or negativity).[30] Alsheikh *et al* found that low grade papillary tumours, including PUNLMP, showing a normal CK20 expression pattern recurred less frequently than did those lesions with an abnormal pattern of staining.[11] However, the differences were not significant. In particular, 20% of tumours that were classified as PUNLMP and that recurred showed normal CK20 expression. A similar observation was made by Desai *et al*.[29] The conclusion of these studies was that it was not possible to identify a subset of low grade papillary tumours with a high likelihood of recurrence.

To improve the discrimination between recurrent and non-recurrent cases, some attempts were made to investigate the predictive role of the combined expression of CK20 with either the high molecular weight cytokeratin 34βE12[31] or with CD44.[29] CD44 encompasses a family of polymorphic transmembrane glycoproteins involved in cell surface binding to hyaluronidase, collagen, fribronectin, and ankyrin.[13 15 29] The combined immunoprofile of CK20 and 34βE12 was analysed by Ramos *et al*.[15] They concluded that CK20 and the 34βE12 antigen were strong predictive markers of disease recurrence when considering different topographic expression profiles.[15] CD44 expression was evaluated by Desai *et al*,[29] who found that CK20 and CD44 did not show a significant correlation with recurrence.

Other studies evaluated proliferative activity, either alone or in association with other markers, such as p53, c-erbB-2, and bcl-2.[8 13 14 31] Proliferation was measured either as MIB-1 expression or as mitotic count. The limitations of these studies and of those mentioned in the previous paragraphs are that the markers were evaluated by a variety of assays, using a variety of reagents, interpreted according to variable criteria, and reported in a variable manner.

However, such studies basically agree on the fact that p53 expression is uncommon in PUNLMP and is often present in low grade papillary carcinoma, whereas proliferative activity is increased in PUNLMP compared with benign urothelium, and this increase is more pronounced in low grade papillary carcinoma. Pich *et al* showed that MIB-1 immunopositivity was the only independent factor predicting disease recurrence.[8] The same group of authors also performed a rather simple morphometric analysis of the nuclear area and perimeter. They found no close relation between these two features and recurrence.

> ''Our study shows that karyometry can be used to plan follow up strategies in patients with papillary urothelial neoplasm of low malignant potential lesions, predict the results of therapeutic interventions, and categorise patients into risk groups''

In recent times, more comprehensive karyometric analyses have been performed.[16 17 32] These included the evaluation of nuclear chromatin texture. Gschwendtner *et al* showed that nuclear texture feature analysis is capable of distinguishing between normal and neoplastic urothelial nuclei, with the performance of this approach being superior to DNA ploidy analysis.[32] A similar technique was used in a study carried out by our group,[16] and we found that karyometry detected an abnormal chromatin pattern and distribution in the normal looking urothelium adjacent to papillary carcinoma. Such alterations correspond to so called malignancy associated changes. Both studies applied such an analysis to cases still classified on the basis of the 1973 WHO scheme, and did not investigate the relation between texture feature changes and disease recurrence, even though the existence of an association between the chromatin pattern and prognosis was suggested.

Van Velthoven *et al* investigated the role of quantitative chromatin pattern analysis in the identification of patients at risk for recurrence.[17] They based their study on the 1973 WHO classification. Patients with either non-invasive (pTa) or lamina propria invasive (pT1) disease (superficial bladder cancer) were considered. They found that discriminant analysis based on chromatin texture features (related to chromatin distribution and condensation) was more efficient in determining the risk of recurrence than the conventional grading and staging systems.

Our present karyometric study differs from the previous one in that it is based on the current grading system (1998 WHO/ISUP; that is, the 2004 WHO classification) and non-invasive PUNLMP lesions only were investigated.[16 17 32 33] Its sample size of 20 provided 80% statistical power to identify classification algorithms as performing significantly better than chance if their true accuracy rates were 80% or higher, a reasonable demand if the usefulness of this approach is to be demonstrated. The results of our study went against our original expectations: it had been considered unlikely that nuclei collected from biopsies of PUNLMP lesions would provide prognostic information as to which cases might have a recurrence. Similar to the previous studies,[16 17] it has been shown that nuclear chromatin texture features are superior to those concerning nuclear area and DNA content when those patients who experience disease recurrence have to be identified.

Our study shows that karyometry can be used to plan follow up strategies in patients with PUNLMP lesions, predict the results of therapeutic interventions, elucidate the natural history of cancer, and, in particular, categorise patients into risk groups. In addition to this, karyometry has a role in detecting the minor differences existing between PUNLMP and urothelial papilloma—a lesion that is usually thought to be benign and to require a follow up strategy different from that of the other papillary lesions.

Little is known about the underlying biological mechanisms responsible for the subvisual differences in chromatin organisation state between non-recurrent and recurrent cases. The fact that the patterns of chromatin packaging are consistent within defined pathological groups may be considered an indication of functional interrelations between nuclear structure and gene expression,[34] and suggests that chromatin organisation is under very tight cellular control

Take home messages

- Karyometry and multivariate analyses detect subvisual differences in the chromatin organisation state between non-recurrent and recurrent urothelial papillary neoplasms of low malignant potential—the chromatin granules in the recurrent group are darker and larger
- This approach can be used to predict whether or not the lesions will recur
- Further studies using a larger sample, in which a proliferation marker could also be evaluated, should be conducted to estimate more precisely the accuracy of the classification algorithms presented here, and to provide a statistical analysis of the sensitivity and specificity of this approach

and that chromatin phenotype impacts on malignant potential. Epigenetic mechanisms such as histone acetylation and methylation probably play a major role in determining the chromatin pattern. Many recent studies have also shown that nuclear architecture, higher order chromatin organisation, and the topology of chromosomal territories in interphase cells might be involved in gene regulation.[35] A comprehensive model for these interactions does not yet exist but, as our study shows, the nuclear chromatin phenotype provides very specific clues to the underlying pathology, and its study is likely to be extremely important in cancer pathobiology.

In conclusion, karyometry and multivariate analyses detect subvisual differences in chromatin organisation state between non-recurrent and recurrent urothelial papillary neoplasms of low malignant potential (the chromatin granules in the recurrent group are not only darker, but larger), thus allowing a prediction of whether or not the lesions will recur. Similar analyses conducted in a larger sample, in which a proliferation marker could also be evaluated, will enable us to estimate more precisely the accuracy of the classification algorithms presented here, in addition to providing a statistical analysis of the sensitivity and specificity of this approach.

ACKNOWLEDGEMENTS

This research has been supported by grants from the Polytechnic University of the Marche Region (Ancona, Italy) (MS), the Italian Ministry of University and Scientific Research (RM, 2003), and, in part, by a grant from the National Cancer Institute, CA 53877–13 (PHB). The content of this paper is solely the responsibility of the authors and does not necessarily represent the official views of the Polytechnic University of the Marche Region (Ancona, Italy) or the National Cancer Institute (USA). We wish to thank Ms D Thompson, Tucson, Arizona, USA, for her valuable assistance in image recording and feature analysis.

Authors' affiliations

M Scarpelli, R Montironi, L M Tarquini, Section of Pathological Anatomy and Histopathology, Polytechnic University of the Marche Region, I-60020 Ancona, Italy
P W Hamilton, The Queen's University, Belfast BT 12 6BL, Northern Ireland, UK
A López Beltran, Unit of Anatomic Pathology, Cordoba University Medical School, Cordoba 14071, Spain
J Ranger-Moore, College of Public Health, Arizona Cancer Center, University of Arizona, Tucson, AZ85721, USA
P H Bartels, Optical Sciences Center, University of Arizona

REFERENCES

1 **Epstein JI**, Amin MB, Reuter VR, *et al*. The bladder consensus conference committee: the World Health Organization/International Society of Urological Pathology consensus classification of urothelial (transitional cell) neoplasms of urinary bladder. *Am J Surg Pathol* 1998;**22**:1435–48.
2 **Mostofi FK**, Sorbin LH, Torloni H. Histological typing of urinary bladder tumours. *International classification of tumours, 19*. Geneva: World Health Organisation, 1973.
3 **Bostwick DG**, Lopez-Beltran A. *Bladder biopsy interpretation*. New York: United Pathologist Press, 1999.
4 **Bostwick DG**, Mikuz G. Urothelial papillary (exophytic) neoplasms. *Virchows Arch* 2002;**441**:109–16.
5 **Busch C**, Algaba F. The WHO/ISUP 1998 and WHO 1999 systems for malignancy grading of bladder cancer. Scientific foundation and translation to one another and previous systems. *Virchows Arch* 2002;**441**:105–8.
6 **Montironi R**, Lopez-Beltran A, Mazzucchelli R, *et al*. Classification and grading of the non-invasive urothelial neoplasms: recent advances and controversies. *J Clin Pathol* 2003;**56**:91–5.
7 **Holmäng S**, Hedelin H, Anderström C, *et al*. Recurrence and progression in low-grade papillary urothelial neoplasms. *J Urol* 1999;**162**:702–7.
8 **Pich A**, Chiusa L, Formiconi A, *et al*. Proliferative activity is the most significant predictor of recurrence in non-invasive papillary urothelial neoplasms of low malignant potential and grade 1 papillary carcinomas of the bladder. *Cancer* 2002;**95**:784–90.
9 **Cheng L**, Neumann RM, Bostwick DG. Papillary urothelial neoplasms of low malignant potential. Clinical and biologic implications. *Cancer* 1999;**86**:2102–8.
10 **Samaratunga H**, Makarov DV, Epstein JI. Comparison of WHO/IUSP and WHO classification of non-invasive papillary urothelial neoplasms for risk of progression. *Urology* 2002;**60**:315–19.
11 **Alsheikh A**, Mohamedali Z, Jones E, *et al*. Comparison of the WHO/IUSP classification and cytokeratin 20 expression in predicting the behavior of low-grade papillary urothelial tumors. *Mod Pathol* 2001;**14**:267–72.
12 **Edwards J**, Duncan P, Going JJ, *et al*. Identification of loci associated with putative recurrence genes in transitional cell carcinoma of the urinary bladder. *J Pathol* 2002;**196**:380–5.
13 **Helpap B**, Köllermann J. Assessment of basal cell status and proliferative patterns in flat and papillary lesions: a contribution to the new WHO classification of urothelial tumors of the urinary bladder. *Hum Pathol* 2000;**31**:745–50.
14 **Pich A**, Chiusa L, Formiconi A, *et al*. Biologic differences between non-invasive papillary urothelial neoplasms of low malignant potential and low-grade (grade 1) papillary carcinomas of the bladder. *Am J Surg Pathol* 2001;**25**:1528–33.
15 **Ramos D**, Navarro S, Villamón R, *et al*. Cytokeratin expression patterns in low grade papillary urothelial neoplasms of the urinary bladder. *Cancer* 2003;**97**:1876–83.
16 **Montironi R**, Scarpelli M, Mazzucchelli R, *et al*. Subvisual changes in chromatin organization state are detected by karyometry in the histologically normal urothelium in patients with synchronous papillary carcinoma. *Hum Pathol* 2003;**34**:893–901.
17 **van Velthoven R**, Petein M, Oosterlinck W, *et al*. Identification by quantitative chromatin pattern analysis of patients at risk for recurrence of superficial transitional bladder carcinoma. *J Urol* 2000;**164**:2134–7.
18 **Bahr GF**, Bartels PH, Bibbo M, *et al*. Evaluation of the Papanicolaou stain for computer assisted cellular pattern recognition. *Acta Cytol* 1973;**17**:106–12.
19 **Keenan S**, Diamond J, McCluggage G, *et al*. Nuclear chromatin texture in the grading of cervical intraepithelial neoplasia (CIN). *Cytometry Suppl* 2002;**11**:116A.
20 **Haralick RM**, Shamugam K, Dinstein I. Textural features for image classification. *IEEE Trans Syst Man Cybernet* 1973;**3**:610–21.
21 **Young T**, Verbeek PW, Mayall B. Characterization of chromatin distributions in cell nuclei. *Cytometry* 1986;**7**:467–74.
22 **Bartels PH**, Montironi RM, Bostwick D, *et al*. Karyometry of secretory cell nuclei in high-grade PIN lesions. *Prostate* 2001;**48**:144–55.
23 **Kruskal WH**, Wallis WA. Use of ranks on one-criterion variance analysis. *J Am Stat Assoc*. 1952;47: 583–621, [Addendum:1953;**48**:907–11.].
24 **Bartels PH**, Olson GB. Computer analysis of lymphocyte images. In: Catsimpoolas N, eds. *Methods of cell separation*, Vol. 3. New York: Plenum Press, 1980:1–99.
25 **Beale EMI**. Euclidean cluster analysis. *Bulletin of the International Statistics Institute* 1969;**43**:21–43.
26 **StataCorp**. *Stata Statistical Software: Release 8.2*. College Station, TX: Stata Corporation, 2003.
27 **Cooley WW**, Lohnes PR. Classification procedures. In: Cooley WW, Lohnes PR, eds. *Multivariate data analysis*. New York: John Wiley, 1971:262–86.
28 **Bartels PH**, Duval da Silva V, Montironi R, *et al*. Chromatin texture signature in nuclei from prostate lesions. *Anal Quant Cytol Histol* 1998;**20**:407–16.
29 **Desai S**, Lim SD, Jimenez EJ, *et al*. Relationship of cytokeratin 20 and CD44 protein expression with WHO/ISUP grade in pTa and pT1 papillary urothelial neoplasia. *Mod Pathol* 2000;**13**:1315–23.
30 **Harnden P**, Allam A, Joyce AD, *et al*. Cytokeratin 20 expression by non-invasive transitional cell carcinomas: potential for distinguishing recurrent from non-recurrent disease. *Histopathology* 1995;**27**:169–74.
31 **Cina SJ**, Lancaster-Weiss K, Lecksell K, *et al*. Correlation of Ki-67 and p53 with the new World Health Organization/International Society of Urological Pathology classification system for urothelial neoplasia. *Arch Pathol Lab Med* 2001;**125**:646–51.
32 **Gschwendtner A**, Hoffmann-Weltin Y, Mikuz G, *et al*. Quantitative assessment of bladder cancer by nuclear texture analysis using automated high-resolution image cytometry. *Mod Pathol* 1999;**12**:806–13.
33 **Montironi R**, Scarpelli M, Sisti S, *et al*. Quantitative analysis and malignancy progression of the papillary neoplasia of urinary bladder. *Pathol Res Pract* 1987;**182**:528–9.
34 **Zini N**, Trimarchi C, Claudio PP, *et al*. pRb2/p130 and p107 control cell growth by multiple strategies and in association with different compartments within the nucleus. *J Cell Physiol* 2001;**189**:34–44.
35 **Cremer T**, Cremer C. Chromosome territories, nuclear architecture and gene regulation in mammalian cells. *Nat Rev Genet* 2001;**2**:292–301.

Karyometry detects subvisual differences in chromatin organisation state between non-recurrent and recurrent papillary urothelial neoplasms of low malignant potential

M Scarpelli, R Montironi, L M Tarquini, P W Hamilton, A López Beltran, J Ranger-Moore and P H Bartels

J Clin Pathol 2004 57: 1201-1207
doi: 10.1136/jcp.2004.017608

Notes